

ENHANCING THE ABSORPTION OF RUTIN AND EFFECTIVE CANCER MANAGEMENT THROUGH HYALURONIC ACID FUNCTIONALIZED NANOPARTICLES

S. SRI BHUVANESWARI^{ID}, D. KUMUDHA*^{ID}

¹Department of Pharmacy, Karpagam Academy of Higher Education, Coimbatore-641021, Tamil Nadu, India

*Corresponding author: D. Kumudha; *Email: kumudhachem@gmail.com

Received: 27 Feb 2024, Revised and Accepted: 27 May 2024

ABSTRACT

Objective: The objective of this study is to develop Rutin Nanoparticles (RTN) and coat them with Hyaluronic Acid (HA) to overcome rutin's solubility and bioavailability limitations, and to enhance its uptake by cancer cells through selective delivery mechanisms.

Methods: RTN were synthesized employing soya lecithin and chitosan through the homogenization technique. To further enhance the delivery of rutin to cancer cells, the optimized nanoparticle formulation was coated with HA to enhance its accumulation in cancer cells. The nanoparticles were characterized in terms of particle size (PS) distribution, zeta potential (ZP), entrapment efficiency (EE), morphology, *in vitro* drug release and *in vitro* cytotoxicity activities.

Results: The resulting RTN and HA-coated RTN (HA RTN) exhibited particle sizes of 202.8 nm and 714 nm, with Polydispersity index (PDI) values of 26.4% and 25.5%, respectively. These findings suggest favourable stability and potential for cellular uptake. Moreover, *in vitro* examinations of drug release showcased a prolonged release pattern consistent with the Higuchi kinetic model, indicating a mechanism where drug release is primarily governed by diffusion. The *in vitro* cytotoxicity assay revealed that the HA RTN formulation demonstrated superior efficacy in inhibiting MCF-7 cells compared to free rutin and the uncoated RTN, as evidenced by the respective IC₅₀ values of 145 µg, 342 µg, and 413 µg.

Conclusion: These findings highlight the promising potential of the HA RTN formulation as an effective anti-cancer treatment, paving the way for further development and clinical application of rutin-loaded nanoparticles in cancer therapy.

Keywords: Nanoparticles, Cancer cell, Rutin, RTN and HA RTN

© 2024 The Authors. Published by Innovare Academic Sciences Pvt Ltd. This is an open access article under the CC BY license (<https://creativecommons.org/licenses/by/4.0/>) DOI: <https://dx.doi.org/10.22159/ijap.2024v16i4.50749> Journal homepage: <https://innovareacademics.in/journals/index.php/ijap>

INTRODUCTION

The increasing focus on natural active ingredients has garnered significant interest in various fields, including nutraceuticals, cosmetics, pharmaceuticals, and medical research. Rutin, a natural flavonoid abundantly present in various natural sources, has gained attention due to its potential protective role against diseases associated with oxidative stress [1-3]. Its effectiveness in countering numerous cancers has been attributed to its diverse mechanisms of action, including cell cycle arrest, inflammation suppression, inhibition of malignant cell growth, induction of apoptosis, modulation of angiogenesis and regulation of cellular signaling pathways [4]. However, rutin exhibits low *in vivo* bioavailability, possibly attributable to its chemical structure, particularly glycosylation at the C3 position. Additionally, rutin's inherently low water solubility presents a challenge [5]. To address these limitations, various delivery systems for rutin have been investigated [6, 7]. The attributes of these delivery systems, including substantial surface area, sustained drug release, superior cellular uptake, and the ability to enhance solubility and drug bioavailability, make them particularly suitable, especially for lipophilic drugs [8, 9]. Incorporating rutin into nanoparticles represents a promising strategy to address its solubility and bioavailability limitations. Furthermore, the selective delivery of HA to cancer cells, achieved via the enhanced permeability and retention (EPR) effect, represents a significant advancement. Additionally, HA's interaction with specific receptors, such as CD44 and LYVE-1, which are involved in HA-mediated motility, significantly contributes to augmenting its targeting abilities [9, 10]. Coating or conjugating nanoparticles with HA can significantly augment the availability of the drug at cancer cells [11]. In this study, we have developed nanoparticles of rutin and subsequently coated them with HA. This innovative approach aims to overcome the solubility and bioavailability challenges associated with rutin and enhance its uptake by cancer cells.

MATERIALS AND METHODS

Rutin, soya lecithin and chitosan were purchased from Ioba Chemie Pvt. Ltd, (Mumbai, India); HA was obtained from carbanio; dialysis membrane (MW 12,000–14,000 D) was obtained from HiMedia, (Mumbai, India).

Compatibility study

In this study, Fourier-Transform Infrared Spectroscopy (FTIR) analysis was employed to investigate potential interactions among rutin, soya lecithin, chitosan, and HA present in the formulation. The analysis was conducted across a wavelength range from 400 cm⁻¹ to 4000 cm⁻¹, aiming to discern any observable interactions between these components [12].

Preparation of RTN

RTN were prepared by molecular self-assembly using soya lecithin and chitosan. Initially, a solution of soya lecithin was prepared in 96% ethanol. The nanoparticle formulation was prepared through the combination of a lecithin-rutin-ethanol solution (4 ml) with a chitosan solution (46 ml) using plastic needle tubing with an internal diameter of 0.4 mm. The chitosan solution was made by dissolving chitosan in 50 ml of distilled water, supplemented with 3% acetic acid. This emulsion was subjected to mechanical agitation at 10,000 rpm for a duration of 15 min using an OMNI Mixer homogenizer. The resulting lecithin-chitosan nanoparticles suspension was subjected to centrifugation at 19,000 rpm for 60 min at 4 °C, resulting in the separation and removal of the supernatant. The sediment was resuspended in 5 ml of deionized water and subjected to centrifugation once again. This double centrifugation process was repeated, after which the nanoparticles were subjected to lyophilization for a period of 48 h. 3% dextrose was used as a cryoprotectant during the lyophilization process. Finally, the lyophilized nanoparticles were stored at -20 °C until further use (table 1) [13, 14].

Table 1: Formulation of RTN

Trial	Rutin (mg)	Ratio	
		Soya lecithin	Chitosan
T1	5 mg	1	10
T2	5 mg	1	15
T3	5 mg	1	20
T4	5 mg	1	25
T5	5 mg	1	30
T6	5 mg	1	32
T7	5 mg	1	38
T8	5 mg	1	40
T9	5 mg	1	44
T10	5 mg	1	48
T11	5 mg	1	50
T12	5 mg	1	54

Preparation of HA RTNs

The HARTN formulation was prepared using the electrostatic attraction technique. In a nutshell, 1 ml of a 0.02% (w/v) solution of HA (300 kDa) was meticulously introduced with continuous stirring (20000 rpm) into a dispersion of RTN, maintaining a weight ratio of 12:1. Subsequently, the formulation was lyophilized and stored at a temperature of 4 °C [16].

Evaluation of HA RTNs

Entrapment efficiency (EE) and drug loading

The EE of the RTN dispersion was assessed using the centrifugation method as described by reference. Specifically, RTN with an equivalent amount of 5 mg of the rutin was subjected to centrifugation at 20,000 rpm for 1 h in a centrifuge (REMI motors) in order to separate the supernatant liquid. Subsequently, the liquid was filtered, and the concentration of free rutin was determined after appropriate dilution with a fresh phosphate buffer saline (PBS) at pH 7.4. The UV spectrophotometer was utilized to measure the absorbance at 207 nm [15].

Particle size, zeta potential and surface morphology

The particle size (PS) distribution analysis and zeta potential (ZP) of RTN and HA RTN was conducted through laser scanning utilizing Anton Paar litesizer DLS 500 instrument, following proper dilution with distilled water. This assessment provided data on the mean PS, PDI and ZP. The zeta ZP plays a crucial role in assessing the charges present on the particle surface, offering insights into the sustained stability of the formulation. Meanwhile, the PDI parameter characterizes the extent of dispersity in the lipid nanoparticle dispersions. It is imperative to attain a minimal PDI value, as higher dispersity leads to greater mass scattering [17, 18].

To analyse the surface morphology of HA RTN, a scanning electron microscope (SEM) (SE S-3400N; HITACHI, Japan) was employed. For this examination, lyophilized HA RTNs were securely affixed to the metal surface using double-sided adhesive tape. Subsequently, all samples underwent a gold-palladium (Au-Pd) coating before being examined under vacuum conditions at 5 kV [19].

In vitro drug release

The study of HA RTN was conducted at 37 °C using the dialysis bag method, with 200 ml of PBS and ethanol in a ratio of 65:35 serving as the dialysis medium. The experiment was carried out with continuous agitation at a fixed rate of 100 rpm. A precisely measured quantity of freeze-dried HA RTN (equivalent to 5 mg) was placed inside a dialysis bag with a 10 kDa molecular weight cut-off. Samples of the release medium were collected at various time points over a period of 48h. After each sampling, 1 ml of the solution taken out was substituted with an equivalent volume of the new medium to maintain a consistent sink condition. The quantity of rutin in the solution was assessed via UV-Vis spectrophotometry at a wavelength of 207 nm [20-22]. All experiments were conducted in triplicate.

In vitro cytotoxicity assay

The study investigated the cytotoxicity effects and safety of rutin, RTN and HA RTN using an *in vitro* (3-[4,5-dimethylthiazol-2-yl]-2,5 diphenyl tetrazolium bromide) (MTT) assay. For *in vitro* cytotoxicity assessment, Michigan Cancer Foundation-7 (MCF-7) Cells (1×10^4) were seeded in individual wells of a 96-well plate and incubated for 48 h under 5% CO₂ at 37 °C. Subsequently, the cells were exposed to varying concentrations (20, 30, 50, 100, 150, 200, and 300 µg/ml) of pure rutin, RTN and HA RTN for a duration of 72 h. When cells reached 70% confluence, MTT reagent (10µL, at a final concentration of 0.5 mg/ml) was introduced into each well and incubated for 4 h. Afterwards, acidified isopropanol, serving as the MTT destaining solution (100 µl), was added and the solution was agitated for 15 min [23-25]. Ultimately, the determination of optical density at the 570 nm wavelength was conducted using a microplate reader.

RESULTS AND DISCUSSION

Compatibility study

FTIR analysis was employed to investigate the intermolecular interactions and compatibility among the lipids, HA, and Rutin. In the FTIR spectrum of soy lecithin, the peaks at 3346.27 and 1739.67 correspond to O-H bending and C=O stretching, respectively. Additionally, the peaks observed at 1234.36 and 1068.49 are attributed to the presence of C-O and C-C bonds within the soy lecithin molecule [26]. Chitosan showed its characteristic peaks at 3305.76 associated to N-H and O-H stretching and 2881 attributed to C-H stretching, 1664.45 corresponds to C=O stretching [27]. In the identification spectrum of Rutin, peaks at 1654.81 and 1456.16 indicate aromatic C-H bending and C=O stretching, respectively. Additionally, the peak at 808.12 signifies C=C bending in Rutin [28]. The characteristic peaks of HA were identified at 1606.59 (amide C=O stretching), 3314.44 (N-H stretching), 3045 (O-H stretching), and 1554.52 (C-O stretching) [29]. The physical mixture was observed with the characteristic peaks of individual components, indicating no interaction between the components in the nanoparticle preparation (fig. 1-5).

Preparation of nanoparticles

Nanoparticles were prepared by molecular self-assembly method using soya lecithin and chitosan. The ratio of soya lecithin to chitosan was fixed based on the entrapment efficacy of the prepared RTNs. The soya lecithin to chitosan ratio of 38:1 (T7) was found to have the maximum entrapment efficacy.

Entrapment efficacy

Trials T1 and T2 failed to provide the EE data, potentially due to formulation or experimental variables. With an increase in the ratio of soya lecithin to chitosan, a substantial enhancement in drug EE was observed, culminating in a peak of 91.12% in trial T7. However, as the ratio exceeded a certain threshold (T8 and beyond), there was a decline in EE, indicating the existence of an optimal range for the soya lecithin to chitosan ratio [30]. Trail T7 with maximum EE was selected for H A coating (table 2).

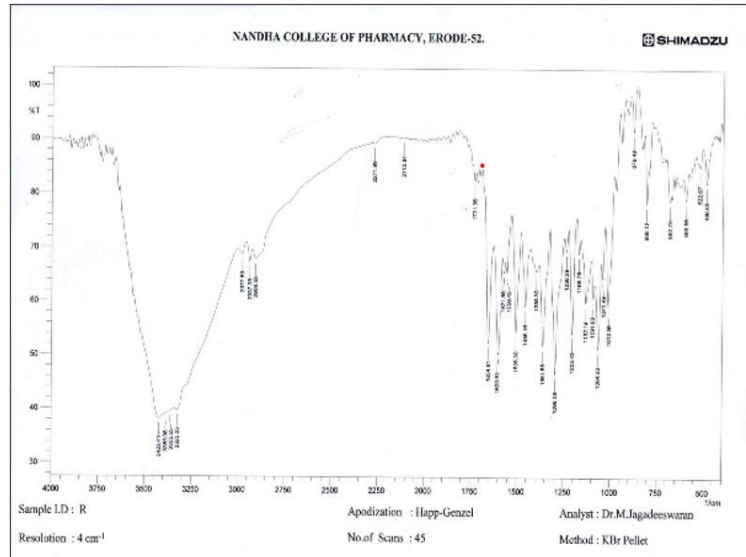


Fig. 1: FTIR of soya lecithin

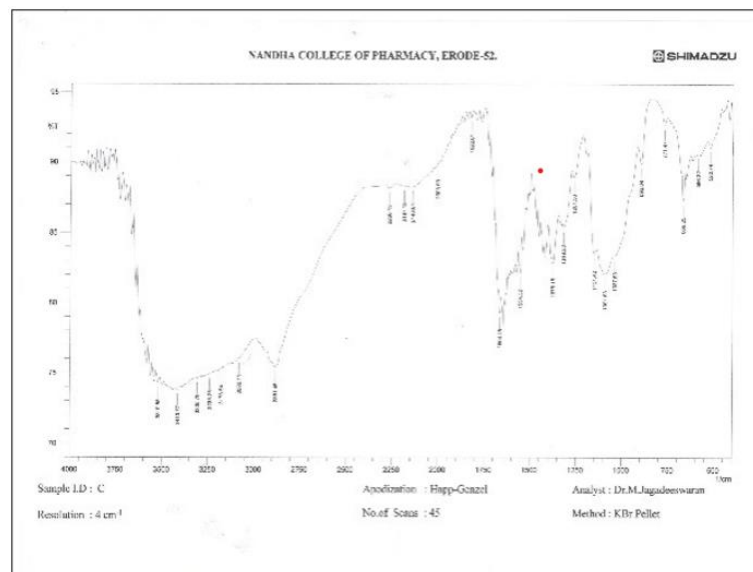
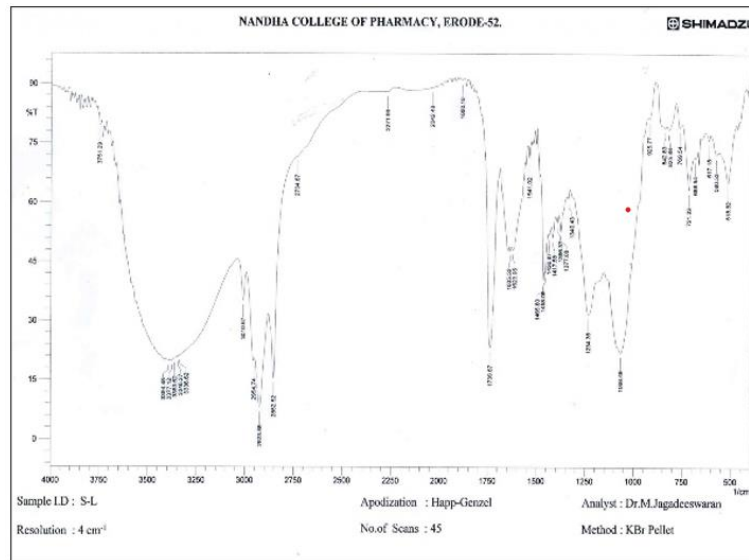


Fig. 2: FTIR of rutin

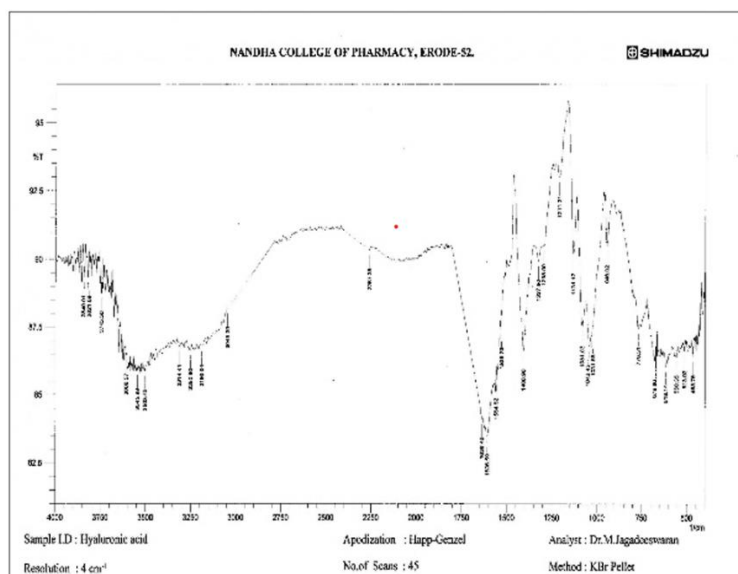


Fig. 3: FTIR of HA

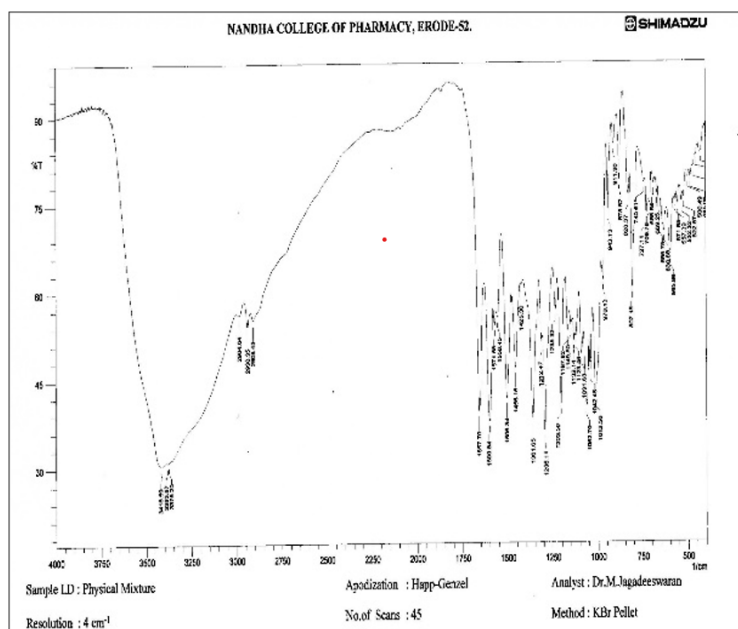


Fig. 4: FTIR of physical mixture

Table 2: EE of prepared RTN

Trial	Entrapment efficacy
T1	—
T2	—
T3	24.73±0.032
T4	36.11±0.046
T5	68.44±0.025
T6	70.86±0.013
T7	91.12±0.021
T8	69.42±0.087
T9	67.17±0.098
T10	66.50±0.063
T11	54.91±0.045
T12	49.14±0.071

value are expressed as mean±SD, Number of experiments, n=3

Particle size, PDI and zeta potential

The PS of RTN and HA RTN were determined to be 202.8 nm and 714 nm, respectively (fig. 6,8). The PDI values were 26.4% and 25.5% for RTN and HA RTN, indicating a narrow distribution width and confirming a uniform PS distribution, demonstrating high dispersion quality. ZP measurement is crucial for predicting the

storage stability of colloidal particles, as charged particles are less prone to aggregation. The measured ZP were -0.0124V and -0.003V, indicating a negative charge on the particle surface (fig. 7,9). The combination of low PDI values and slightly negative ZP suggests that the chosen method for preparing nanoparticle, along with the incorporation of HA coating, was well-suited for the formulation of these nanoparticles [31, 32].

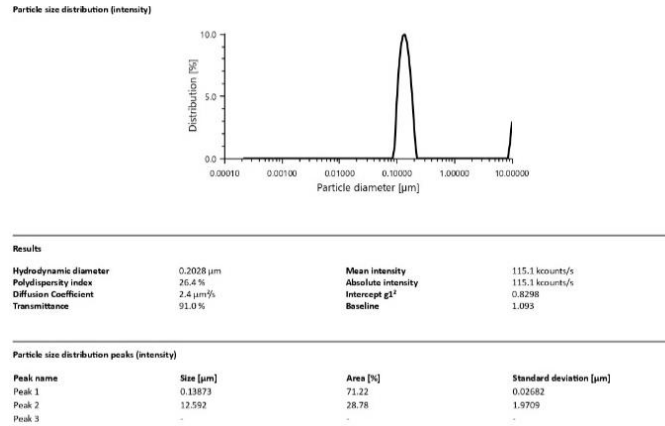


Fig. 6: PS and PDI of RTN

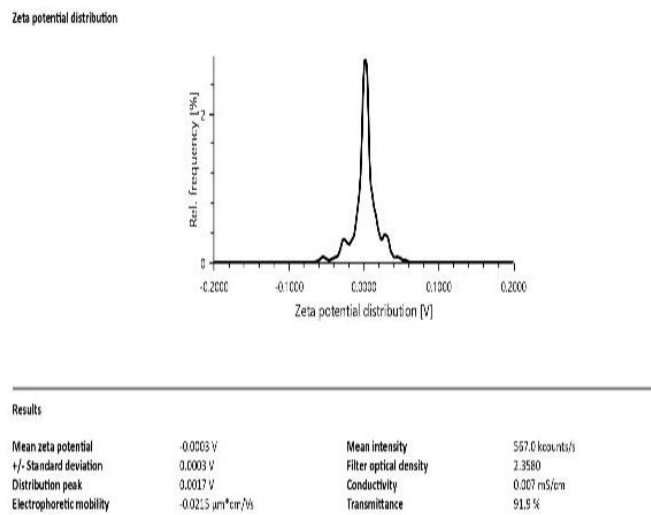


Fig. 7: ZP of RTN

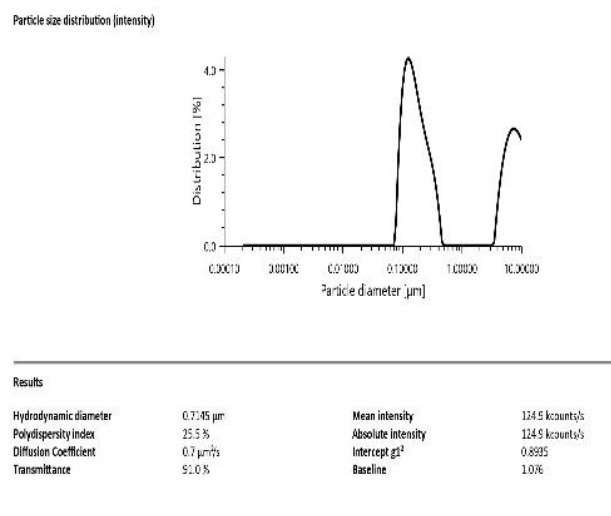


Fig. 8: PS and PDI of HA RTN

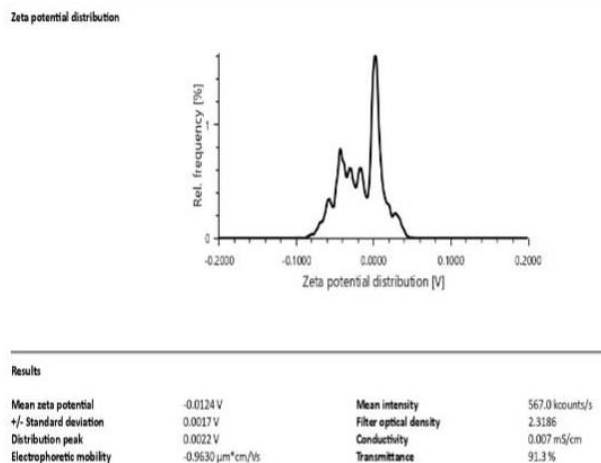


Fig. 9: ZP of HA RTN

Scanning electron microscopy

SEM analysis revealed that the RTN and HA RTN exhibited a spherical morphology characterized by a smooth surface, as depicted in fig. 10 and 11 (A and B), respectively.

In vitro drug release

In vitro study provided valuable understanding into the behaviour of HA RTN. As illustrated in fig. 12, the cumulative release from RTN and HA RTN exhibited a prolonged release pattern over time. The optimized batch RTN and HA RTN drug release profile demonstrated a significant increase from an initial content of $15.36 \pm 1.47\%$ to final

concentration of $96.73 \pm 1.01\%$ and $12.61 \pm 1.60\%$ to a final content of $94.95 \pm 2.43\%$ respectively. This observed gradual release can be attributed to the effective diffusion of the drug through the lipid core of the nanoparticles [33, 34].

The analysis of the data involved the application of various models, including zero-order, first-order, the Higuchi model and the Korsmeyer-Peppas model. The optimized batch, Higuchi's model exhibited the highest correlation coefficient ($R^2=0.9807$), followed by the Korsmeyer-Peppas model (0.9781), first-order ($R^2=0.9756$), Hixon Crowell model (0.9745) and zero-order ($R^2=0.8525$) models, as illustrated in the (table 3) (fig. 13-17).

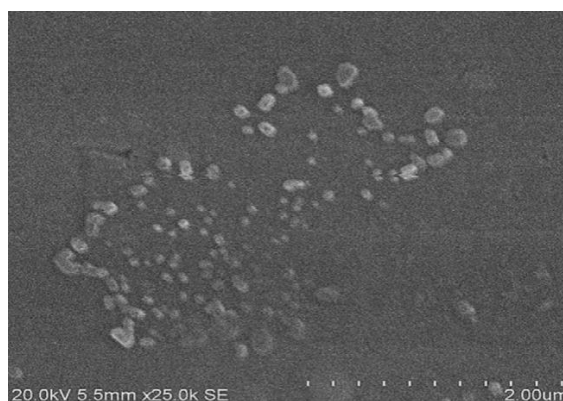


Fig. 10: SEM image of RTN (Magnification: X5000 and X10,000)

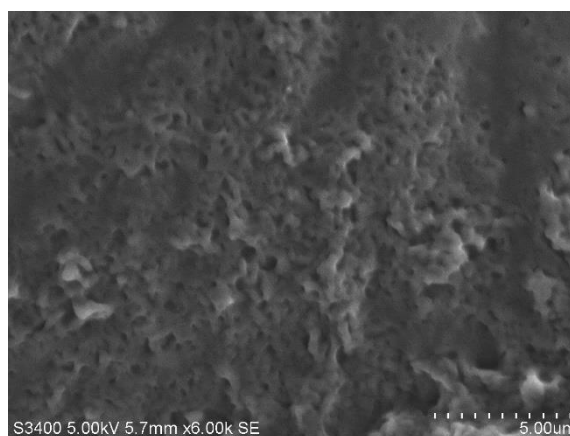


Fig. 11A: SEM image of HA RTN (Magnification X 5000)

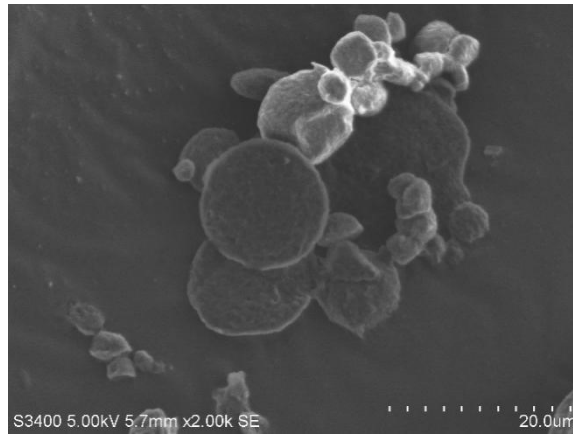


Fig. 11B: SEM image of HA RTN (Magnification X 10,000)

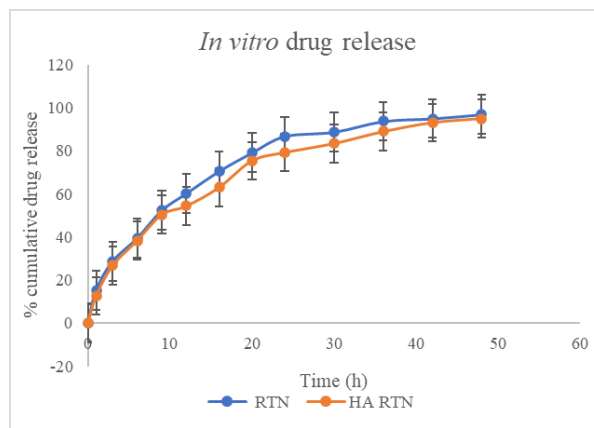


Fig. 12: Cumulative % drug release, IC₅₀ values were expressed as mean±SD, with the number of experiments, n=3

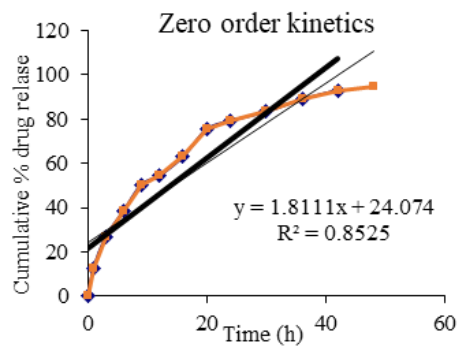


Fig. 13: Zero order drug release kinetics

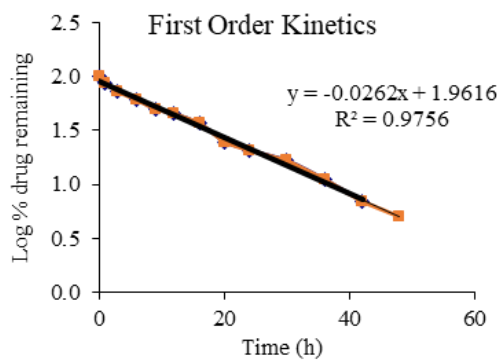


Fig. 14: First-order drug release kinetics

Table 3: Regression coefficients from release data

Release kinetics	Zero order model	First order model	Higuchi model	Korsmayer peppas model	Hixon Crowell model
R ² value	0.8525	0.9756	0.9807	0.9781	0.9745

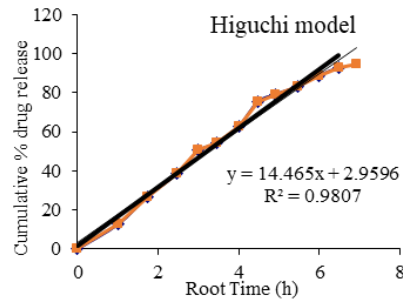


Fig. 15: Higuchi model drug release kinetics

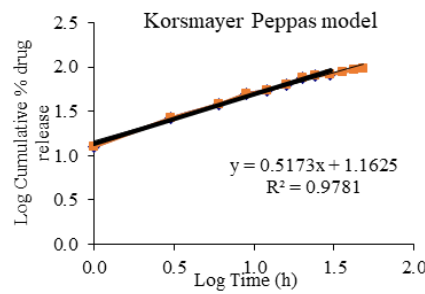


Fig. 16: Kors Mayer Peppas model drug release kinetics

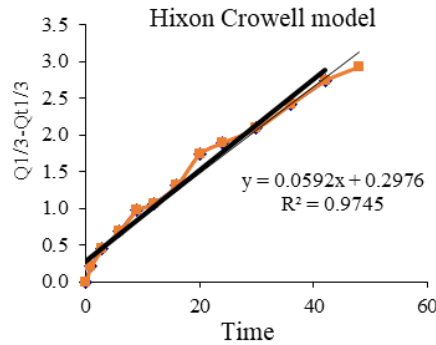


Fig. 17: Hixon Crowell model drug release kinetics

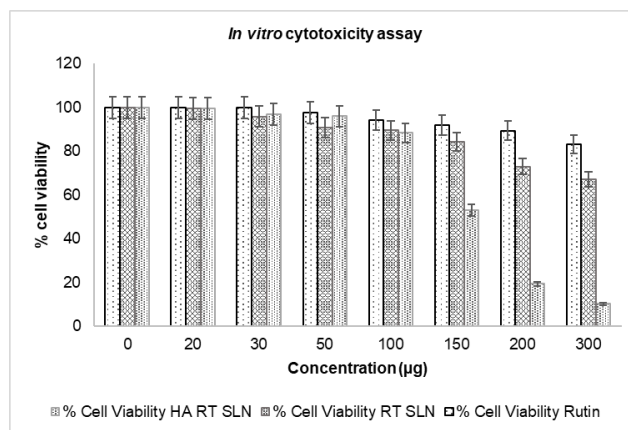


Fig. 18: In vitro cytotoxicity assay, IC50 values were expressed as mean ± SD, with the number of experiments, n=3

CONCLUSION

In conclusion, our study successfully developed and characterized HA RTN for enhanced delivery to cancer cells. The formulation exhibited favourable physicochemical properties, with a PS of 714 nm, PDI of 25.5%, and a ZP of -0.0124V, ensuring stability and potential for cellular uptake. The *in vitro* investigations on drug release exhibited a prolonged release pattern, aligning with the principles of the Higuchi kinetic model, suggesting a mechanism for drug release predominantly governed by diffusion. Significantly, the cytotoxicity assay revealed the superior efficacy of HA RTN in inhibiting MCF-7 cancer cells compared to free rutin and uncoated formulation (RTN). The IC₅₀ values for HA RTN, RTN, and rutin were 145 µg/ml, 342 µg/ml, and 413 µg/ml, respectively. These results highlight the promising potential of the developed HA RTN formulation as an effective anti-cancer treatment, addressing the solubility and bioavailability challenges associated with rutin. This innovative approach of combining nanoparticles with HA coating demonstrates a synergistic strategy for targeted drug delivery, offering a foundation for further development and potential clinical applications of HARTN in cancer therapy.

ACKNOWLEDGEMENT

We would like to express our sincere gratitude to Karpagam Academy of Higher education and research. Special thanks to research team for their invaluable guidance and insightful discussions that greatly contributed to shaping this research.

FUNDING

Nil

AUTHORS CONTRIBUTIONS

Dr. D. Kumudha: She is a research guide and principal under his noble guidance; this article has been prepared.

S. Sri Bhuvaneswari: She has contributed to designed the study, interpretation of results and writing the manuscript. Both authors read and approved the final manuscript.

CONFLICT OF INTERESTS

Declared none

REFERENCES

- Ganeshpurkar A, Saluja AK. The pharmacological potential of Rutin. *Saudi Pharm J.* 2017;25(2):149-64. doi: 10.1016/j.jsps.2016.04.025, PMID 28344465.
- Prasad R, Prasad SB. A review on the chemistry and biological properties of Rutin, a promising nutraceutical agent. *Asian J Pharm Pharmacol.* 2019;5Suppl 1:1-20. doi: 10.31024/ajpp.2019.5.s1.1.
- Pivec T, Kargl R, Maver U, Bracic M, Elschner T, Zagar E. Chemical structure-antioxidant activity relationship of water-based enzymatic polymerized rutin and its wound healing potential. *Polymers.* 2019;11(10):1566. doi: 10.3390/polym11101566, PMID 31561552.
- Kopustinskiene DM, Jakstas V, Savickas A, Bernatoniene J. Flavonoids as anticancer agents. *Nutrients.* 2020;12(2):457. doi: 10.3390/nu12020457, PMID 32059369.
- Choi SS, Park HR, Lee KA. A comparative study of rutin and rutin glycoside: antioxidant activity, anti-inflammatory effect, effect on platelet aggregation and blood coagulation. *Antioxidants (Basel).* 2021;10(11):1696. doi: 10.3390/antiox10111696, PMID 34829567.
- Mishra V, Bansal KK, Verma A, Yadav N, Thakur S, Sudhakar K. Solid lipid nanoparticles: emerging colloidal nano drug delivery systems. *Pharmaceutics.* 2018;10(4):191. doi: 10.3390/pharmaceutics10040191, PMID 30340327.
- De Gaetano F, Cristiano MC, Venuti V, Crupi V, Majolino D, Paladini G. Rutin-loaded solid lipid nanoparticles: characterization and *in vitro* evaluation. *Molecules.* 2021;26(4):1039. doi: 10.3390/molecules26041039, PMID 33669321.
- Sivadasan D, Ramakrishnan K, Mahendran J, Ranganathan H, Karuppaiah A, Rahman H. Solid lipid nanoparticles: applications and prospects in cancer treatment. *Int J Mol Sci.* 2023;24(7):6199. doi: 10.3390/ijms24076199, PMID 37047172.
- Dosio F, Arpicco S, Stella B, Fattal E. Hyaluronic acid for anticancer drug and nucleic acid delivery. *Adv Drug Deliv Rev.* 2016;97:204-36. doi: 10.1016/j.addr.2015.11.011, PMID 26592477.
- Song JM, Im J, Nho RS, Han YH, Upadhyaya P, Kassie F. Hyaluronan-CD44/RHAMM interaction-dependent cell proliferation and survival in lung cancer cells. *Mol Carcinog.* 2019;58(3):321-33. doi: 10.1002/mc.22930, PMID 30365189.
- Huang G, Huang H. Application of hyaluronic acid as carriers in drug delivery. *Drug Deliv.* 2018;25(1):766-72. doi: 10.1080/10717544.2018.1450910, PMID 29536778.
- Yassin AE, Anwer MK, Mowafy HA, El-Bagory IM, Bayomi MA, Alsarra IA. Optimization of 5-fluorouracil solid-lipid nanoparticles: a preliminary study to treat colon cancer. *Int J Med Sci.* 2010;7(6):398-408. doi: 10.7150/ijms.7.398, PMID 21103076.
- Sonvico F, Cagnani A, Rossi A, Motta S, Di Bari MT, Cavatorta F. Formation of self-organized nanoparticles by lecithin/chitosan ionic interaction. *Int J Pharm.* 2006;324(1):67-73. doi: 10.1016/j.ijpharm.2006.06.036, PMID 16973314.
- Perez Ruiz AG, Ganem A, Olivares Corichi IM, Garcia Sanchez JR. Lecithin-chitosan-TPGS nanoparticles as nanocarriers of (-)-epicatechin enhanced its anticancer activity in breast cancer cells. *RSC Adv.* 2018;8(61):34773-82. doi: 10.1039/c8ra06327c, PMID 35547028.
- Onugwu AL, Attama AA, Nnamani PO, Onugwu SO, Onuigbo EB, Khutoryanskiy VV. Development and optimization of solid lipid nanoparticles coated with chitosan and poly(2-ethyl-2-oxazoline) for ocular drug delivery of ciprofloxacin. *J Drug Deliv Sci Technol.* 2022;74:103527. doi: 10.1016/j.jddst.2022.103527.
- Shen H, Shi S, Zhang Z, Gong T, Sun X. Coating solid lipid nanoparticles with hyaluronic acid enhances antitumor activity against melanoma stem-like cells. *Theranostics.* 2015;5(7):755-71. doi: 10.7150/thno.10804, PMID 25897340.
- Siram K, Karuppaiah A, Gautam M, Sankar V. Fabrication of hyaluronic acid surface modified solid lipid nanoparticles loaded with imatinib mesylate for targeting human breast cancer MCF-7 cells. *J Clust Sci.* 2023;34(2):921-31. doi: 10.1007/s10876-022-02265-y.
- Shrivastava S, Kaur CD. Development of andrographolide-loaded solid lipid nanoparticles for lymphatic targeting: formulation, optimization, characterization, *in vitro*, and *in vivo* evaluation. *Drug Deliv Transl Res.* 2023;13(2):658-74. doi: 10.1007/s13346-022-01230-6, PMID 35978260.
- Adeyemi SA, Az-Zamakhshariy Z, Choonara YE. *In vitro* prototyping of a nano-organogel for thermo-sonic intra-cervical delivery of 5-fluorouracil-loaded solid lipid nanoparticles for cervical cancer. *AAPS Pharm Sci Tech.* 2023;24(5):123. doi: 10.1208/s12249-023-02583-y, PMID 37226039.
- Rahman MA, Ali A, Rahamathulla M, Salam S, Hani U, Wahab S. Fabrication of sustained release curcumin-loaded solid lipid nanoparticles (cur-SLNs) as a potential drug delivery system for the treatment of lung cancer: optimization of formulation and *in vitro* biological evaluation. *Polymers.* 2023;15(3):542. doi: 10.3390/polym15030542, PMID 36771843.
- Korake S, Bothiraja C, Pawar A. Design, development, and *in vitro/in vivo* evaluation of docetaxel-loaded PEGylated solid lipid nanoparticles in prostate cancer therapy. *Eur J Pharm Biopharm.* 2023;189:15-27. doi: 10.1016/j.ejpb.2023.05.020, PMID 37270157.
- Jain A, Vyas SP. Formulation and characterization of gdl-based artesunate solid lipid nanoparticle. *Int J App Pharm.* 2023;15(5):68-74. doi: 10.22159/ijap.2023v15i5.48913.
- Homayouni Tabrizi MH, Soltani M, Es-haghi A. Preparation and characterization of the farnesiferol C-loaded solid lipid nanoparticles decorated with folic acid-bound chitosan and evaluation of its *in vitro* anti-cancer and anti-angiogenic activities. *J Mol Liq.* 2023;382:121908. doi: 10.1016/j.molliq.2023.121908.
- Ghasemi M, Turnbull T, Sebastian S, Kempson I. The MTT assay: utility, limitations, pitfalls, and interpretation in bulk and single-cell analysis. *Int J Mol Sci.* 2021;22(23):12827. doi: 10.3390/ijms222312827, PMID 34884632.

25. Hatami M, Kouchak M, Kheirollah A, Khorsandi L, Rashidi M. Quercetin-loaded solid lipid nanoparticles exhibit antitumor activity and suppress the proliferation of triple-negative MDA-MB 231 breast cancer cells: implications for invasive breast cancer treatment. *Mol Biol Rep.* 2023;50(11):9417-30. doi: 10.1007/s11033-023-08848-w, PMID 37831347.
26. Suryavanshi A, Kumar S, Arya DK. Evaluation of phytochemical and antibacterial potential of *Ajuga parviflora* Benth *Med Plnts Int J Phyt Rela Ind.* 2020;12(1):144-9. doi: 10.5958/0975-6892.2020.00019.2.
27. Tariq H, Rehman A, Kishwar F, Raza ZA. Micellar synthesis of lime oil-loaded chitosan microstructures for the sustainable development of antibacterial cellulosic fabric. *Cellulose.* 2023;30(17):11177-94. doi: 10.1007/s10570-023-05469-1.
28. Nandiyanto AB, Oktiani R, Ragadhita R. How to read and interpret FTIR spectroscopy of organic material. *Indonesian J Sci Technol.* 2019;4(1):97-118. doi: 10.17509/ijost.v4i1.15806.
29. Pan NC, Pereira HC, da Silva ML, Vasconcelos AF, Celligoi MA. Improvement production of hyaluronic acid by *Streptococcus zooepidemicus* in sugarcane molasses. *Appl Biochem Biotechnol.* 2017;182(1):276-93. doi: 10.1007/s12010-016-2326-y, PMID 27900664.
30. Shrivastava S, Kaur CD. Development of andrographolide-loaded solid lipid nanoparticles for lymphatic targeting: formulation, optimization, characterization, *in vitro*, and *in vivo* evaluation. *Drug Deliv Transl Res.* 2023;13(2):658-74. doi: 10.1007/s13346-022-01230-6, PMID 35978260.
31. Bibi M, Din F, Anwar Y, Alkenani NA, Zari AT, Mukhtiar M. Cilostazol-loaded solid lipid nanoparticles: bioavailability and safety evaluation in an animal model. *J Drug Deliv Sci Technol.* 2022;74. doi: 10.1016/j.jddst.2022.103581.
32. Parvez S, Karole A, Mudavath SL. Fabrication, physicochemical characterization and *in vitro* anticancer activity of nerolidol encapsulated solid lipid nanoparticles in human colorectal cell line. *Colloids Surf B Biointerfaces.* 2022;215:112520. doi: 10.1016/j.colsurfb.2022.112520, PMID 35489319.
33. De Gaetano F, Celesti C, Paladini G, Venuti V, Cristiano MC, Paolino D. Solid lipid nanoparticles containing morin: preparation, characterization, and *ex vivo* permeation studies. *Pharmaceutics.* 2023;15(6):1605. doi: 10.3390/pharmaceutics15061605, PMID 37376054.
34. Stella B, Peira E, Dinzani C, Gallarate M, Battaglia L, Gigliotti CL. Development and characterization of solid lipid nanoparticles loaded with a highly active doxorubicin derivative. *Nanomaterials (Basel).* 2018;8(2). doi: 10.3390/nano8020110, PMID 29462932.
35. Perez Ruiz AG, Ganem A, Olivares Corichi IM, Garcia Sanchez JR. Lecithin-chitosan-TPGS nanoparticles as nanocarriers of (-)-epicatechin enhanced its anticancer activity in breast cancer cells. *RSC Adv.* 2018;8(61):34773-82. doi: 10.1039/c8ra06327c, PMID 35547028.
36. Kis B, Pavel IZ, Avram S, Moaca EA, Herrero San Juan M, Schwiebs A. Antimicrobial activity, *in vitro* anticancer effect (MCF-7 breast cancer cell line), antiangiogenic and immunomodulatory potentials of *Populus nigra* L. buds extract. *BMC Complement Med Ther.* 2022;22(1):74. doi: 10.1186/s12906-022-03526-z, PMID 35296309.
37. Dudhat KR, V Patel HV. Novel nanoparticulate systems for idiopathic pulmonary fibrosis: a review. *Asian J Pharm Clin Res.* 2020 Nov 7;13(11):3-11. doi: 10.22159/ajpcr.2020.v13i11.39035.
38. Datta A, Das A, Ghosh R. Eudragit® R1100 microspheres as a delayed-release system for ibuprofen: *in vitro* evaluation. *Int J Pharm Pharm Sci.* 2024;14(12):6-10. doi: 10.22159/ijpps.2022v14i12.45838.
39. Arumugam K, D Borawake P, Shinde JV. Formulation and evaluation of floating microspheres of ciprofloxacin by solvent evaporation method using different polymers. *Int J Pharm Pharm Sci* 2021;13(7):101-8. doi: 10.22159/ijpps.2021v13i7.41204.
40. Shivalingam MR, Balasubramanian A, Ramalingam K. Formulation and evaluation of transdermal patches of pantoprazole sodium. *Int J App Pharm.* 2021;13(5):287-91. doi: 10.22159/ijap.2021v13i5.42175.